ARTICLE IN PRESS

Available online at www.sciencedirect.com

ScienceDirect

Mathematics and Computers in Simulation ▮ (▮▮▮▮) ▮▮▮–▮▮▮

MATHEMATICS AND COMPUTERS IN SIMULATION

www.elsevier.com/locate/matcom

Original articles

Minimal modeling methodology to characterize non-linear damping in an electromechanical system

N. Wongvanich, C.E. Hann*, H.R. Sirisena

Department of Electrical and Computer Engineering, University of Canterbury, Private Bag 4800, Ilam, Christchurch, 8140, New Zealand

Received 26 March 2014; received in revised form 29 January 2015; accepted 26 May 2015

Abstract

This paper presents a minimal modeling methodology for capturing highly non-linear dynamics in an electromechanical cart system. A theoretical foundation for the method is given including a proof of identifiability and a numerical example to demonstrate the theory. The second order differential equation model describing the cart system is reformulated in terms of integrals to enable a fast method for identification of both constant and time varying parameters. The model is identified based on a single experimental proportional step response and is validated on a proportional–derivative (PD) controlled step input for a range of gains. Two models with constant damping and time varying non-linear damping were considered. The fitting accuracy for each model was tested on three separate data sets corresponding to three proportional gains. The three data sets gave similar non-linear damping models and in all cases the non-linear model gave smaller fitting errors than the linear model. For the PD control responses, the non-linear model reduced the mean absolute prediction error by a factor of three. The non-linear model also provided significantly better PD control design. These results demonstrate the ability of the proposed method to accurately capture significant non-linearities in the data. Computationally, the proposed algorithm is shown to be significantly faster than standard non-linear regression.

Keywords: Minimal modeling approach; Non-linear damping; Integral method; Electro-mechanical cart system

1. Introduction

Many systems have non-linear oscillatory behavior, for example pitch control of an aircraft [21], building response to seismic load [3,23], robotic arm [6,20], and car suspension control [1,25]. A common approach to analyzing vibration responses in various applications is to assume linear damping and break the responses into various modal frequencies. For example, modal analysis is commonly used for assessing damage of a building after an earthquake [29,13], and for characterizing stability of power systems [17,16,28]. Another common approach is Prony's Analysis [16,24,2], which is similar in concept to the Fourier Transformation, and extracts a series of damped complex exponentials from the signal. Other methods have involved Kalman filter based designs, [31], non-linear regression

* Corresponding author. Tel.: +64 3 364 2987x7242.
E-mail addresses: wongvanich@ieee.org (N. Wongvanich), chris.hann@canterbury.ac.nz (C.E. Hann), harsha.sirisena@canterbury.ac.nz (H.R. Sirisena).

http://dx.doi.org/10.1016/j.matcom.2015.05.007

Please cite this article in press as: N. Wongvanich, et al., Minimal modeling methodology to characterize non-linear damping in an electromechanical system, Math. Comput. Simulation (2015), http://dx.doi.org/10.1016/j.matcom.2015.05.007

analysis [19,22], and statistical methods such as the Mean-Likelihood estimator [14], to estimate the damping coefficient.

In electro-mechanical systems, significant non-linear damping exists, including static friction and gear backlash [32]. The usual approach to capturing this phenomena is to have a pre-assumed non-linear representation, for example, the Bingham viscoplastic model, assumes that the force of the damper is a given non-linear function of the damper velocity [26], and the Bouc–Wen model includes a model describing hysteric behavior of the damper [30]. There are also several models of gear backlash [15,5]. Thus, the concept is to start with complex model structures first, and then fit it to the data. If required, more complex models of damping can be used including finite elements [18,12].

This research presents a different philosophy by starting with initially simplified structures for the model then using correlations between the time varying parameters and measured data to "bootstrap" a more complex and accurate non-linear model. In this paper a general non-linear modeling approach to damping in second-order systems is presented. The approach is based on a time-varying damping formulation which is proven in theory and applied to an electromechanical cart system. The method identifies a general damping profile under continuity constraints so avoids any potentially incorrect assumptions on the precise nature of the non-linear damping present. Furthermore, this approach allows an integral based method for parameter identification to be developed that linearizes the optimization problem. This identification method has been validated in biomedical applications which tend to involve coupled first order systems [11,8,27,9], and rocket roll dynamics which are overdamped and first order [10]. The extension to second order systems is not straightforward as dynamics can be significantly oscillatory and initial conditions involve derivatives. This paper includes the extension of this method to both second order and non-linear parameters, and provides a proof of the theoretical convergence and identifiability of this nonlinear modeling approach. Although, this paper is primarily on the non-linear characterization and comparison with linear models, this extended integral method is important in terms of minimizing computational requirements for the non-linear identification. The second order non-linear model is identified on a closed-loop response and is shown to accurately capture the system non-linear dynamics over a wide range of inputs. The non-linear model is shown to be significantly more accurate than a model with linear damping, and thus provides better control system prediction and design.

2. Methodology

2.1. Spring–mass–damper with time-varying damping

The differential equation for a linear spring is defined:

$$m\ddot{y} + c\ddot{y} + ky = u(t) \tag{1}$$

where $y \equiv y(t)$ is the displacement (m), $u(t)$ the input force (N), m the mass (kg), c the damping factor (kg/s), and k the stiffness of the spring N/m. For the case of free vibration where $u(t) = 0$, without loss of generality it can be assumed that $m = 1$, and thus Eq. (1) is written in the form:

$$\ddot{y} + c\dot{y} + ky = 0 \tag{2}$$

$$\text{initial conditions} \equiv y(0) = y_0, \quad y'(0) = dy_0. \tag{3}$$

Eqs. (2) and (3) describe the transient response of a spring–mass–damper which is useful for modeling the dynamics of single degree of freedom systems, for example electro-mechanical systems [32]. In practice, the damping c in Eq. (2) is often non-linear and can include dynamics of both static and dynamic friction and gear backlash [32,26,5]. The approach presented in this paper is to treat the damping c initially as time-varying then relating it to measured quantities like velocity and displacement. In other words, the philosophy is to use a simplified model to bootstrap more complex models to capture the measured response.

To allow flexibility in the model, a constant piecewise model of damping is used. Hence, Eq. (2) is rewritten in the form:

$$\ddot{y} + c(t)\dot{y} + ky = 0 \tag{4}$$

Please cite this article in press as: N. Wongvanich, et al., Minimal modeling methodology to characterize non-linear damping in an electromechanical system, Math. Comput. Simulation (2015), http://dx.doi.org/10.1016/j.matcom.2015.05.007

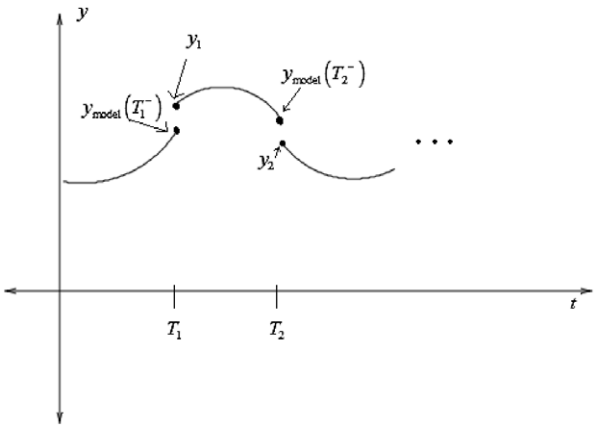

Fig. 1. Discontinuity of $y_{\text{model},i}(t)$ defined in Eq. (11).

where:

$$\begin{aligned} c(t) &= c_1, \quad T_0 < t < T_1 \\ &= \vdots \\ &= c_n \quad T_{n-1} < t < T_{end} \end{aligned} \tag{5}$$

$$T_{i+1} - T_i = \Delta t, \quad i = 0, \ldots, n-1 \tag{6}$$

$$T_0 = 0, \quad \Delta t \equiv \text{user defined time interval}, \quad N = \text{number of damping values}. \tag{7}$$

2.2. Integral method — time varying damping

To identify $\{c_i, i = 1, \ldots, n\}$ and k in Eqs. (4) and (5), an integral based approach is used. The concept was first developed on first order differential equations [10], and in this section is extended to second order differential equations. Eq. (4) is first double integrated over time from T_{i-1} to $t \in [T_{i-1}, T_i]$, which yields:

$$y(t) - y_{i-1} - \alpha_{i-1}(t - T_{i-1}) + c_i \int_{T_{i-1}}^{t} y_m \mathrm{d}t + k \int_{T_{i-1}}^{t} \int_{T_{i-1}}^{t} y_m \mathrm{d}t \mathrm{d}t = 0 \tag{8}$$

where:

$$y_{i-1} = y(T_{i-1}), \quad y'_{i-1} = y'(T_{i-1}), \quad i = 1, \ldots, n \tag{9}$$

$$\alpha_{i-1} = y'_{i-1} + c_i y_{i-1}. \tag{10}$$

The initial conditions of Eq. (9) are defined at the beginning of each interval that the time-varying damping of Eq. (5) is defined over.

Let $y_m(t)$ denote measured data in the system described by Eqs. (4) and (5). Define the function:

$$\begin{aligned} y_{\text{model},i}(t) &= y_{i-1} + \alpha_{i-1}(t - T_{i-1}) - c_i \int_{T_{i-1}}^{t} y_m \mathrm{d}t - k \int_{T_{i-1}}^{t} \int_{T_{i-1}}^{t} y_m \mathrm{d}t \mathrm{d}t, \\ & i = 1, \ldots n, \quad t \in [T_{i-1}, T_i). \end{aligned} \tag{11}$$

The initial conditions in Eq. (11) are initially considered as unknown parameters and may not necessarily correspond to measured data points. Furthermore, for arbitrary values of these initial conditions, the function in Eq. (11) could be discontinuous. Fig. 1 demonstrates this scenario with arrows pointing to the discontinuities in the y_i values. Similarly there are discontinuities in the y'_i values but for clarity, these are not shown. To enforce C^1 continuity so that the

Please cite this article in press as: N. Wongvanich, et al., Minimal modeling methodology to characterize non-linear damping in an electromechanical system, Math. Comput. Simulation (2015), http://dx.doi.org/10.1016/j.matcom.2015.05.007

scenario in Fig. 1 cannot occur, the following equality constraints are defined:

$$y_{\text{model},i}(T_i^-) = y_i, \quad y'_{\text{model},i}(T_i^-) = y'_i, \quad i = 1, \ldots, n. \tag{12}$$

Eq. (12) provides $2n - 2$ equations that can uniquely identify the $2n - 2$ unknown initial conditions $\{y_1, \ldots, y_{n-1}, \alpha_1, \ldots, \alpha_{n-1}\}$.

Choose N equally spaced time points $\{t_1^{(i)}, \ldots, t_N^{(i)}\}$ in each interval $[T_{i-1}, T_i)$, $i = 1, \ldots, n$. Setting $y_{\text{model}}(t) = y_m(t)$ for $t \in \{t_1^{(i)}, \ldots, t_N^{(i)}, i = 1, \ldots, n\}$ gives a set of nN equations in $3n + 1$ unknown parameters $\{y_0, \ldots, y_{n-1}, \alpha_0, \ldots, \alpha_{n-1}, c_1, \ldots, c_n, k\}$ which is defined by the matrix equation:

$$\mathbf{A}\,\mathbf{a} = \mathbf{b} \tag{13}$$

where:

$$\mathbf{a} = [y_0, \ldots, y_{n-1}, \alpha_0, \ldots, \alpha_{n-1}, c_1, \ldots, c_n, k]^T \tag{14}$$

$$\mathbf{A} = \left[\mathbf{I}_{\mathbf{1}_{\mathbf{N}\times\mathbf{1}}} \mid \mathbf{I}_{\overline{\mathbf{T}}_{\mathbf{N}\times\mathbf{1}}} \mid \mathbf{MM}\right], \quad \mathbf{b} = \begin{bmatrix} {\beta_{\mathbf{N}\times\mathbf{1}}}^{(1)} \\ {\beta_{\mathbf{N}\times\mathbf{1}}}^{(2)} \\ \vdots \\ {\beta_{\mathbf{N}\times\mathbf{1}}}^{(n)} \end{bmatrix}, \tag{15}$$

$${\beta_{\mathbf{N}\times\mathbf{1}}}^{(i)} = \begin{bmatrix} y_m(t_1^{(i)}) \\ \vdots \\ y_m(t_N^{(i)}) \end{bmatrix}, \quad i = 1, \ldots, n$$

$$\mathbf{I}_{\mathbf{V}} = \begin{bmatrix} \mathbf{V} & \mathbf{O}_{\mathbf{N}\times\mathbf{1}} & \ldots & \mathbf{O}_{\mathbf{N}\times\mathbf{1}} \\ \mathbf{O}_{\mathbf{N}\times\mathbf{1}} & \mathbf{V} & \ldots & \mathbf{O}_{\mathbf{N}\times\mathbf{1}} \\ \vdots & \vdots & \ddots & \ldots \\ \mathbf{O}_{\mathbf{N}\times\mathbf{1}} & \mathbf{O}_{\mathbf{N}\times\mathbf{1}} & \ldots & \mathbf{V} \end{bmatrix}, \quad \mathbf{V} = \mathbf{1}_{\mathbf{N}\times\mathbf{1}} \quad \text{or} \quad {\overline{\mathbf{T}}_{\mathbf{N}\times\mathbf{1}}}^{(i)}, \quad i = 1, \ldots, n \tag{16}$$

$$\mathbf{MM} = \begin{bmatrix} {\bar{\mathbf{I}}_{\mathbf{N}\times\mathbf{1}}}^{(1)} & \mathbf{O}_{\mathbf{N}\times\mathbf{1}} & \cdots & \mathbf{O}_{\mathbf{N}\times\mathbf{1}} & {\bar{\mathbf{J}}_{\mathbf{N}\times\mathbf{1}}}^{(1)} \\ \mathbf{O}_{\mathbf{N}\times\mathbf{1}} & {\bar{\mathbf{I}}_{\mathbf{N}\times\mathbf{1}}}^{(2)} & \cdots & \mathbf{O}_{\mathbf{N}\times\mathbf{1}} & {\bar{\mathbf{J}}_{\mathbf{N}\times\mathbf{1}}}^{(2)} \\ \vdots & \vdots & \ddots & \vdots & \vdots \\ \mathbf{O}_{\mathbf{N}\times\mathbf{1}} & \mathbf{O}_{\mathbf{N}\times\mathbf{1}} & \ldots & {\bar{\mathbf{I}}_{\mathbf{N}\times\mathbf{1}}}^{(n)} & {\bar{\mathbf{J}}_{\mathbf{N}\times\mathbf{1}}}^{(n)} \end{bmatrix} \tag{17}$$

$${\bar{\mathbf{I}}_{\mathbf{N}\times\mathbf{1}}}^{(i)} = \begin{bmatrix} -\int_{T_{i-1}}^{t_1^{(i)}} y_m \mathrm{d}t \\ \vdots \\ -\int_{T_{i-1}}^{t_N^{(i)}} y_m \mathrm{d}t \end{bmatrix}, \quad {\bar{\mathbf{J}}_{\mathbf{N}\times\mathbf{1}}}^{(i)} = \begin{bmatrix} -\int_{T_{i-1}}^{t_1^{(i)}} \int_{T_{i-1}}^{t} y_m \mathrm{d}t \mathrm{d}t \\ \vdots \\ -\int_{T_{i-1}}^{t_N^{(i)}} \int_{T_{i-1}}^{t} y_m \mathrm{d}t \mathrm{d}t \end{bmatrix}, \quad i = 1, \ldots, n \tag{18}$$

$$\mathbf{1}_{\mathbf{N}\times\mathbf{1}} \equiv N \times 1 \text{ number of ones}, \quad {\overline{\mathbf{T}}_{\mathbf{N}\times\mathbf{1}}}^{(i)} \equiv \begin{bmatrix} t_1^{(i)} - T_{i-1} \\ \vdots \\ t_N^{(i)} - T_{i-1} \end{bmatrix}, \quad i = 1, \ldots, n \tag{19}$$

$$\mathbf{O}_{\mathbf{N}\times\mathbf{M}} \equiv N \times M \text{ matrix of zeros.} \tag{20}$$

The final algorithm for determining the time varying damping and stiffness in Eq. (4), solves Eqs. (13)–(20) by linear least squares subject to the following equality constraints:

$$\mathbf{A}_{\mathbf{eq}}\,\mathbf{a} = \mathbf{b}_{\mathbf{eq}} \tag{21}$$

Please cite this article in press as: N. Wongvanich, et al., Minimal modeling methodology to characterize non-linear damping in an electromechanical system, Math. Comput. Simulation (2015), http://dx.doi.org/10.1016/j.matcom.2015.05.007

where:

$$\mathbf{A_{eq}} = \left[\begin{array}{c|c|c|c} \mathbf{M_1} & \mathbf{M_2} & \mathbf{M_3} & \mathbf{M_4} \\ \hline \mathbf{O_{n-1\times n}} & \mathbf{M_1} & \mathbf{M_5} & \mathbf{M_6} \end{array}\right] \tag{22}$$

$$\mathbf{M_1} = \begin{bmatrix} 1 & -1 & \cdots & \cdots & 0 & 0 \\ 0 & 1 & -1 & \cdots & 0 & 0 \\ \vdots & \vdots & \ddots & \ddots & \vdots & \vdots \\ 0 & 0 & \cdots & \cdots & 1 & -1 \end{bmatrix}_{(n-1)\times n} \tag{23}$$

$$\mathbf{M_2} = \begin{bmatrix} \Delta t & 0 & \cdots & 0 & 0 \\ 0 & \Delta t & \cdots & 0 & 0 \\ \vdots & \vdots & \ddots & \vdots & \vdots \\ 0 & 0 & \cdots & \Delta t & 0 \end{bmatrix}_{(n-1)\times n} \tag{24}$$

$$\mathbf{M_3} = \begin{bmatrix} -\int_0^{T_1} y_m \mathrm{d}t & 0 & \cdots & 0 & 0 \\ 0 & -\int_{T_1}^{T_2} y_m \mathrm{d}t & \cdots & 0 & 0 \\ \vdots & \vdots & \ddots & \vdots & \vdots \\ 0 & 0 & \cdots & -\int_{T_{n-2}}^{T_{n-1}} y_m \mathrm{d}t & 0 \end{bmatrix}_{(n-1)\times n} \tag{25}$$

$$\mathbf{M_4} = \begin{bmatrix} -\int_0^{T_1}\int_0^{T_1} y_m \mathrm{d}t\,\mathrm{d}t \\ -\int_{T_1}^{T_2}\int_{T_1}^{T_2} y_m \mathrm{d}t\,\mathrm{d}t \\ \vdots \\ -\int_{T_{n-2}}^{T_{n-1}}\int_{T_{n-2}}^{T_{n-1}} y_m \mathrm{d}t\,\mathrm{d}t \end{bmatrix}_{(n-1)\times 1} \tag{26}$$

$$\mathbf{M_5} = \begin{bmatrix} -y_m(T_1) & y_m(T_1) & \cdots & \cdots & 0 & 0 \\ 0 & -y_m(T_2) & y_m(T_2) & \cdots & 0 & 0 \\ \vdots & \vdots & \ddots & \ddots & \vdots & \vdots \\ 0 & 0 & \cdots & \cdots & -y_m(T_{n-1}) & y_m(T_{n-1}) \end{bmatrix}_{(n-1)\times n} \tag{27}$$

$$\mathbf{M_6} = \begin{bmatrix} -\int_0^{T_1} y_m \mathrm{d}t \\ -\int_{T_1}^{T_2} y_m \mathrm{d}t \\ \vdots \\ -\int_{T_{n-2}}^{T_{n-1}} y_m \mathrm{d}t \end{bmatrix}_{(n-1)\times 1} \tag{28}$$

$$\mathbf{b_{eq}} = \mathbf{O_{(2n-2)\times 1}}, \quad \text{where } \mathbf{O_{N\times M}} \text{ is defined in Eq. (20).} \tag{29}$$

The top half of the equality constraints matrix $\mathbf{A_{eq}}$ is associated with the y_i initial conditions, and the bottom half of $\mathbf{A_{eq}}$ is associated with α_{i-1} defined in Eq. (10).

Please cite this article in press as: N. Wongvanich, et al., Minimal modeling methodology to characterize non-linear damping in an electromechanical system, Math. Comput. Simulation (2015), http://dx.doi.org/10.1016/j.matcom.2015.05.007

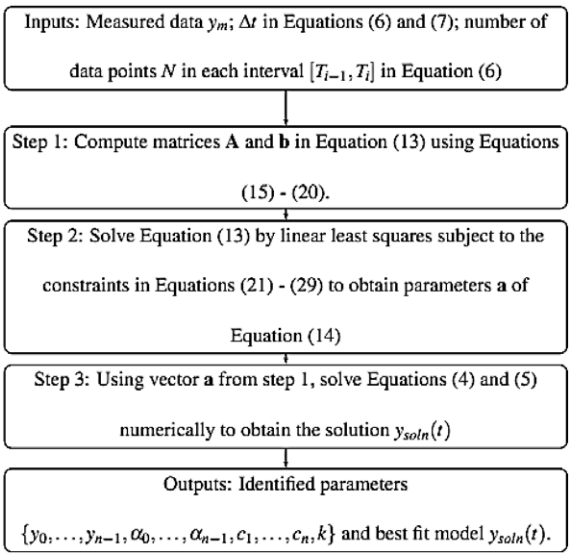

Fig. 2. Algorithm for identifying the time varying damping $c(t)$ and stiffness k in Eq. (4) for a given starting set of initial condition of Eq. (3).

The algorithm is summarized in Fig. 2. Note that the previous integral method [8,27,9] was developed on over-damped systems and only required a single initial condition. For second order systems, the response can be oscillatory and has two initial conditions including the derivative. Furthermore, the time-varying damping is globally constrained over the whole data interval thus requiring a different treatment of the equations compared to [11].

3. Analysis

3.1. Theoretical analysis of model

There is no guarantee that the damping profile obtained from Fig. 2 is unique or physically realistic. For example, consider the following linear time varying damping profile:

$$\ddot{y}_{true} + F_{true}(t)\ \dot{y}_{true} + K y_{true} = 0 \tag{30}$$

$$F_{true}(t) = (0.9 + 0.7\,t), \quad K = 30 \tag{31}$$

$$y_{true}(0) = y_0 = 2, \quad y'_{true}(0) = dy_0 = -1. \tag{32}$$

Fig. 3 shows simulated data from Eq. (30). Choose k intervals $[T_{i-1}, T_i]$, $i = 1, \ldots, k$ and for a given $\epsilon > 0$, define a piecewise model approximation:

$$F_{model,k}(t) = \begin{cases} F_{true}(t) + \dfrac{\epsilon}{(\Delta T)^2\, y'_{true}(t)}, & t \in [0, T_1], \\ F_{true}(t) + \dfrac{2(-1)^{i-1}\epsilon}{(\Delta T)^2\, y'_{true}(t)} & t \in [T_{i-1}, T_i], \quad i = 2, \ldots, k \end{cases} \tag{33}$$

$$T_i = i\,\Delta T, \quad \Delta T = \frac{T_{end}}{k}, \quad T_{end} = 0.55. \tag{34}$$

Double integrating Eq. (30) from 0 to t yields a similar formula to Eq. (11):

$$y_{model,k}(t) = y_0 + dy_0\, t - \int_0^t \int_0^\tau F_{model,k}(s)\, y'_{true}(s)\mathrm{d}t\mathrm{d}t - K \int_0^t \int_0^\tau y_{true}(s)\mathrm{d}s\mathrm{d}\tau. \tag{35}$$

Please cite this article in press as: N. Wongvanich, et al., Minimal modeling methodology to characterize non-linear damping in an electromechanical system, Math. Comput. Simulation (2015), http://dx.doi.org/10.1016/j.matcom.2015.05.007

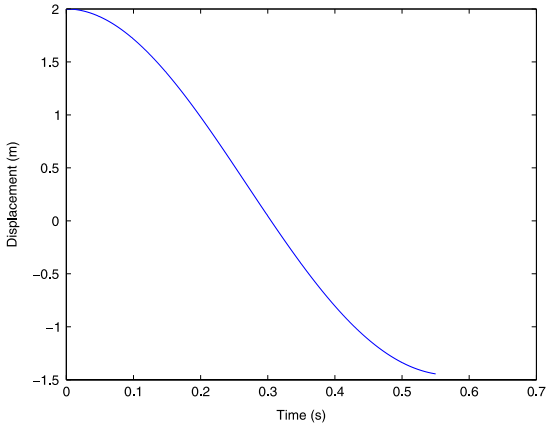

Fig. 3. Simulated data from Eq. (30).

If "model" is replaced by "true" in Eq. (35) the difference between the modeled displacement is:

$$y_{true} - y_{model,k} = \int_0^t \int_0^\tau (F_{model,k}(s) - F_{true}(s)) y'_{true}(s) \mathrm{d}s \mathrm{d}\tau. \tag{36}$$

Substituting Eq. (33) into Eq. (36), double integrating and simplifying yields:

$$y_{true} - y_{model} = \begin{cases} \dfrac{\epsilon}{\Delta T} t, & t \in [0, T_1] \\ = \epsilon - \dfrac{2\epsilon}{\Delta T}(t - T_1), & t \in [T_1, T_2] \\ = -\epsilon + \dfrac{2\epsilon}{\Delta T}(t - T_2), & t \in [T_2, T_3] \\ = (-1)^i \left(\epsilon - \dfrac{2\epsilon}{\Delta T}(t - T_{i-1}) \right), & t \in [T_{i-1}, T_i],\ i = 3, \ldots, k. \end{cases} \tag{37}$$

From Eq. (37), it follows that:

$$|y_{true}(t) - y_{model}(t)| \leq \epsilon, \quad 0 < t \leq T_{end}. \tag{38}$$

Therefore y_{model} can be made arbitrarily close to y_{true}. For any fixed ϵ, as $k \to \infty$, $y_{true}(t)$ remains unchanged and $\Delta T \to 0$ in Eqs. (33)–(34). Thus, the error between F_{model} and F_{true} can be made arbitrarily large.

To approximate Eqs. (33) and (34) for a constant piecewise damping, define $F_{model,k}(t)$ as follows:

$$F_{model,k}(t) = \sum_{i=1}^{k} C^k_{i,model} \Big(H(t - T_{i-1}) - H(t - T_i) \Big), \tag{39}$$

where:

$$C^k_{i,model} = \begin{cases} \bar{c}_{i,true} + \dfrac{\epsilon}{(\Delta T)^2 \bar{dy}_{i,true}}, & i = 1 \\ \bar{c}_{i,true} + \dfrac{2(-1)^{i-1}\epsilon}{(\Delta T)^2 \bar{dy}_{i,true}}, & i = 2, \ldots, k \end{cases} \tag{40}$$

$$\bar{c}_{i,true} = \frac{F_{true}(T_{i-1}) + F_{true}(T_i)}{2}, \quad \bar{dy}_{i,true} = \frac{y'_{true}(T_{i-1}) + y'_{true}(T_i)}{2},$$

$$\Delta T \equiv \frac{T_{end}}{k}, \quad T_{end} = 0.55 \tag{41}$$

and k is the number of equally spaced damping constants chosen between $t = 0$ and $t = T_{end}$.

Please cite this article in press as: N. Wongvanich, et al., Minimal modeling methodology to characterize non-linear damping in an electromechanical system, Math. Comput. Simulation (2015), http://dx.doi.org/10.1016/j.matcom.2015.05.007

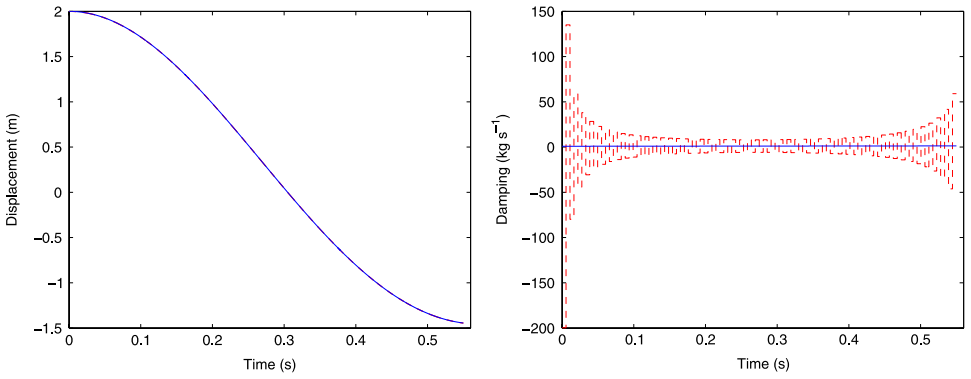

Fig. 4. (a) Model matches to simulated data for $k = 100$ and (b) Comparison of damping model of Eq. (39) to true values for $k = 100$.

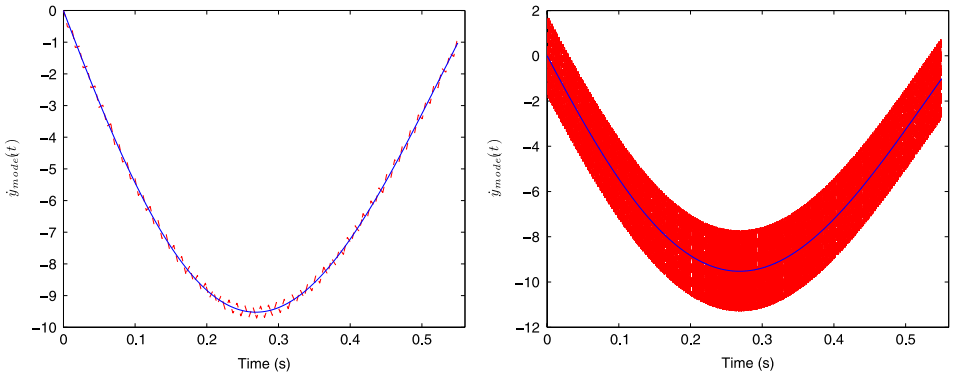

Fig. 5. (a) Comparison of derivative $\dot{y}_{model}(t)$ to true derivative $\dot{y}_{true}(t)$ for $k = 100$ and (b) Comparison of derivative $\dot{y}_{model}(t)$ to true derivative $\dot{y}_{true}(t)$ for $k = 1000$.

The modeled output $y_{model,k}(t)$ can be made arbitrarily close to y_{true} by reducing ϵ in Eqs. (37) and (38). However, as $k \to \infty$ and thus $\Delta T \to 0$ the damping constants in Eq. (40) become unbounded in Eqs. (40)–(41). For example, Fig. 4(a) plots $y_{model,k}(t)$ and $y_{true}(t)$ for $k = 100$. The corresponding damping profile is plotted versus the true damping in Fig. 4(b). Significant oscillations are observed in Fig. 4(b) with large deviations from the true damping, yet the modeled and true curves are very close in Fig. 4(a) with a mean absolute displacement error of 0.001.

The reason for this unboundedness is that the algorithm of Fig. 2 only considers identifying $C(t)$ and does not place a bound on the derivative $C'(t)$ of the resulting modeled profile. There is also no consideration given to the derivative $\dot{y}_{model}(t)$. Figs. 5(a) and (b) plot the comparison between the true derivative curves $\dot{y}_{true}(t)$ versus $\dot{y}_{model}(t)$ for $k = 100$ and $k = 1000$. As k increases, the error in derivative is growing unbounded while the error in the displacement remains less than ϵ.

The example of Figs. 5(a) and (b) motivates the placement of a bound on the derivative of allowable modeled damping profiles, which is expressed in the following theorem and corollary:

Theorem 1. *Consider the following class of second order non-linear differential equations:*

$$\ddot{y}_{true}(t) + F_{true}(t)\ \dot{y}_{true} + K\ y_{true}(t) = 0, \quad t \in [0, T_{end}],$$
$$y_{true}(0) = y_0, \quad \dot{y}_{true}(0) = dy_0, \quad K > 0 \tag{42}$$
$$F_{true}(t) > 0, \quad F_{true} \in C^0, \ \max_{t\in[0,T_{end}]} |\dot{F}_{true}(t)| \ \textit{is finite.} \tag{43}$$

Please cite this article in press as: N. Wongvanich, et al., Minimal modeling methodology to characterize non-linear damping in an electromechanical system, Math. Comput. Simulation (2015), http://dx.doi.org/10.1016/j.matcom.2015.05.007

Define:

$$F_{model,k}(t) = \sum_{i=1}^{k} C_{i,model}^{(k)} \Big(H(t - \Delta t\,(i-1)) - H(t - i\,\Delta t) \Big) \tag{44}$$

$$y_{model,k}(t) = y_0 + dy_0 t - \int_0^t \int_0^t F_{model,k}(t)\, \dot{y}_{true}\, dt\, dt - K \int_0^t \int_0^t y_{true}\, dt\, dt \tag{45}$$

where:

$$H(t - \bar{t}) = \begin{cases} 0, & t < \bar{t}, \\ 1, & t \geq \bar{t} \end{cases} \tag{46}$$

$$\Delta t = \frac{1}{k}, \quad \frac{|C_{i+1,model} - C_{i,model}|}{\Delta t} \leq \alpha, \quad \alpha = \max_{t \in [0, T_{end}]} |\dot{F}_{true}(t)|, \quad i = 1, \ldots, k-1. \tag{47}$$

Choose $C_{i,model}^{(k)}$ *in Eq. (44) so that:*

$$\lim_{n \to \infty} y_{model,n}(t) = y_{true}(t), \quad \forall t \in [0, T_{end}] \tag{48}$$

where $y_{true}(t)$ *is the solution to Eq. (42). The damping profile* $F_{model,k}(t)$ *converges to a unique solution defined by:*

$$\lim_{k \to \infty} F_{model,k}(t) = F_{true}(t), \quad \forall t \in [0, T_{end}] \tag{49}$$

where $F_{true}(t)$ *is the true damping in Eqs. (42) and (43).*

Proof. See proof of theorem 1 in Appendix A. □

Corollary 2. *Let* $C_{i,model}^{*(k)}$, $i = 1, \ldots, k$ *be the linear least squares solution to Eq. (13) with the inequality constraint of Eq. (47) for k intervals. Let* $F_{model}^{*}(t)$ *be the corresponding damping profile with* $C_{i,model}^{(k)} = C_{i,model}^{*(k)}$ *in Eq. (44), then:*

$$\lim_{k \to \infty} F_{model,k}^{*}(t) = F_{true}(t), \quad \forall t \in [0, T_{end}]. \tag{50}$$

Proof. See proof of corollary 1 in Appendix A. □

Corollary 2 shows that the damping profile $F_{true}(t)$ in Eqs. (42) and (43) is uniquely identifiable as the number of intervals k approaches ∞. The key to this result is the inequality constraint in Eq. (47).

3.2. Applying constraints on the integral method

Theorem 1 motivates the use of constraints on the damping values in the algorithm of Fig. 2. These constraints are easy to implement since the non-linear problem has been converted to linear least squares which always has a unique solution and is fast to compute. A physical law can then be derived by relating the identified damping to measurable quantities like velocity or displacement and could include hysteresis if required.

The simplest possible constraint is to put $\alpha = 0$ in Eq. (47) which is equivalent to applying equality constraints $c_1 = c_2 = \cdots = c_n = c$. That is, the damping values are assumed constant across the whole data set. This constraint is important as it allows a comparison of the suitability of more complex models compared to simpler models. In this paper the models are compared in terms of both the fitting error and prediction of control system response in an electro-mechanical cart system. Note that, for the case of constant damping in Eq. (2), the equality constraints of Eqs. (21) and (22) are not required. Setting $y_{model}(t) = y_m(t)$ for $t \equiv \{t_1^{(i)}, \ldots, t_N^{(i)}, i = 1, \ldots, n\}$ gives a set of nN equations in 4 unknowns $\{y_0, \alpha_0, c, k\}$ defined by the matrix equation:

$$\mathbf{A_{const}}\, \mathbf{a_{const}} = \mathbf{b_{const}} \tag{51}$$

Please cite this article in press as: N. Wongvanich, et al., Minimal modeling methodology to characterize non-linear damping in an electromechanical system, Math. Comput. Simulation (2015), http://dx.doi.org/10.1016/j.matcom.2015.05.007

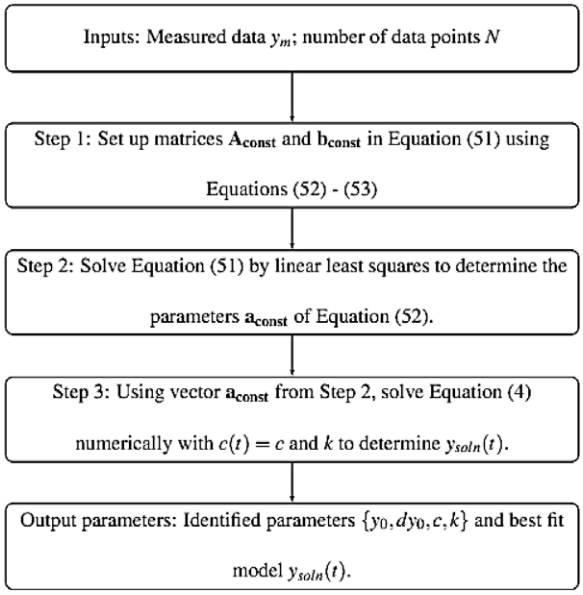

Fig. 6. Algorithm for identifying the time varying damping $c(t)$ and stiffness k in Eq. (4) for a given starting set of initial condition of Eq. (3).

where:

$$\mathbf{A_{const}} = \begin{bmatrix} \mathbf{1_{N\times 1}}^{(1)} & \overline{\mathbf{T}}_{\mathbf{N\times 1}}^{(1)} & \overline{\mathbf{I}}_{\mathbf{N\times 1}}^{(1)} & \overline{\mathbf{J}}_{\mathbf{N\times 1}}^{(1)} \\ \mathbf{1_{N\times 1}}^{(2)} & \overline{\mathbf{T}}_{\mathbf{N\times 1}}^{(2)} & \overline{\mathbf{I}}_{\mathbf{N\times 1}}^{(2)} & \overline{\mathbf{J}}_{\mathbf{N\times 1}}^{(2)} \\ \vdots & \vdots & \vdots & \vdots \\ \overline{\mathbf{1}}_{\mathbf{N\times 1}}^{(n)} & \overline{\mathbf{T}}_{\mathbf{N\times 1}}^{(n)} & \overline{\mathbf{I}}_{\mathbf{N\times 1}}^{(n)} & \overline{\mathbf{J}}_{\mathbf{N\times 1}}^{(n)} \end{bmatrix}, \tag{52}$$

$$\text{`}\mathbf{b_{const}} \equiv \mathbf{b} \text{ in Eq. (15)}, \quad \mathbf{a_{const}} = \begin{bmatrix} y_0 \\ \alpha_0 \\ c \\ k \end{bmatrix}$$

$$\overline{\mathbf{1}}_{\mathbf{N\times 1}}^{(i)}, \quad \overline{\mathbf{T}}_{\mathbf{N\times 1}}^{(i)} \equiv \text{Eq. (19)}, \quad \overline{\mathbf{I}}_{\mathbf{N\times 1}}^{(i)}, \quad \overline{\mathbf{J}}_{\mathbf{N\times 1}}^{(i)} \equiv \text{Eq. (18)}, \quad i = 1, \ldots, n. \tag{53}$$

The algorithm for identifying a constant damping in Eq. (2) is summarized in Fig. 6.

4. Results and discussion

4.1. Parameter identification of an electro-mechanical cart system

4.1.1. Setup and data acquisition

A schematic of the cart system is shown in Fig. 7. The cart can move back and forward along a support rail. The cart is tethered and has two wires, one for the commanded voltage and another for feedback of the cart position which is achieved using an encoder. The origin is set at the middle of the track. The cart system is connected to a space system with Control Desk to allow real-time access to changing control gains, for data acquisition and viewing the signals. A proportional–integral–derivative (PID) controller is designed in Simulink which is then compiled into C code. All data is saved as a `.mat` file in Matlab, and includes the voltage input (V) and cart position (m) which are measured at 1 kHz. The cart is powered by a 12 V DC motor.

Please cite this article in press as: N. Wongvanich, et al., Minimal modeling methodology to characterize non-linear damping in an electromechanical system, Math. Comput. Simulation (2015), http://dx.doi.org/10.1016/j.matcom.2015.05.007

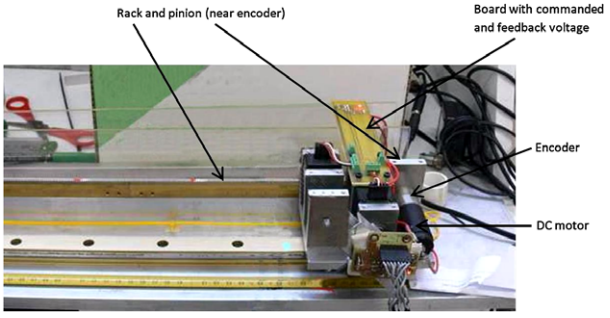

Fig. 7. Electromechanical cart system setup.

4.1.2. Cart modeling

The net force applied to the cart is the force from the input voltage minus the damping force:

$$M\ddot{y} = \alpha_1 V(t) - \alpha_2 \dot{y} \tag{54}$$

where M is mass of cart (kg), $V(t)$ is applied voltage (V), y is cart displacement (m), $\dot{y}$ is cart velocity (m s^{-1}), $\ddot{y}$ is cart acceleration (m s^{-2}), α_1 is the Voltage Constant (N V^{-1}), α_2 is the overall damping (Ns m^{-1}). The damping coefficient C is a lumped parameter which includes armature resistance, friction of the gears and track. The voltage constant includes the gearing ratio and torque constant of the DC motor. Eq. (54) can be rewritten in the form:

$$\ddot{y} = \beta V(t) - C\dot{y} \tag{55}$$

where

$$\beta = \frac{\alpha_1}{M}, \quad C = \frac{\alpha_2}{M} \tag{56}$$

are the normalized voltage constant and damping with respect to mass. The goal of the system identification is to estimate the parameters β and C with minimal experiments to predict control system response. In this paper, a proportional–derivative (PD) controller is considered. For PD control, the voltage $V(t)$ in Eq. (55) is defined:

$$V(t) = K_p e(t) + K_d \dot{e}(t) \tag{57}$$

$$e(t) = r(t) - y(t), \quad r(t) \equiv \text{reference displacement.} \tag{58}$$

The data used is generated by setting $K_d = 0$, and $r(t) = r_0$ which is a closed loop step response. A closed loop response is used for the identification to ensure a stable oscillatory response from the cart. With open loop control there is no feedback to prevent it drifting off course and consequently to the end of the track. Note that open loop tests would always be conducted in the initial design of a system, but eventually the loop must be closed which typically results in many experiments and sophisticated algorithms to obtain the optimal gains. This method is directed towards the tuning stage of the controller and investigates the ability of one closed loop response to characterize all dynamics. A step response has infinitely many sinewaves, so in principle, provides all the dynamics necessary for identification. Furthermore, in some cases, open-loop tests are not possible without causing damage to the system, for example complex tooling in wire fence machines [7].

The goal of the system identification is to identify the parameters β and C in Eq. (55) so that a wide range of step response can be predicted for various gains K_p and K_d without requiring further experiments. For $r(t) = r_0$ in Eq. (58), the model of Eq. (55) is rewritten:

$$-\ddot{e} = \beta(K_p e + K_d \dot{e}) + C\dot{e}. \tag{59}$$

Collecting terms, Eq. (59) becomes:

$$\ddot{e} + \overline{C}\dot{e} + \overline{\beta}e = 0 \tag{60}$$

$$\overline{C} = C + \beta K_d, \quad \overline{\beta} = \beta K_p. \tag{61}$$

Please cite this article in press as: N. Wongvanich, et al., Minimal modeling methodology to characterize non-linear damping in an electromechanical system, Math. Comput. Simulation (2015), http://dx.doi.org/10.1016/j.matcom.2015.05.007

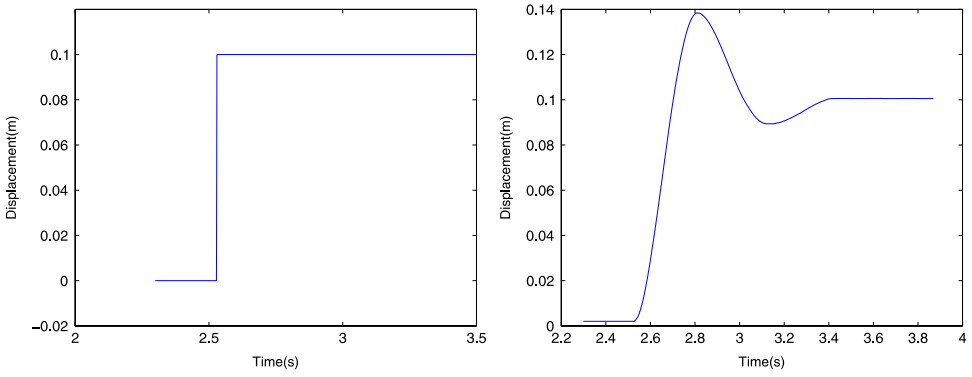

Fig. 8. (a) Reference displacement for cart system and (b) Measured displacement response.

Hence, with PD control the cart system acts as a spring–mass–damper with damping $\overline{C}$ and an analogous "stiffness" of $\overline{\beta}$. Thus, the error $e(t)$ in Eq. (60) acts as a transient response e, and is in the form of Eq. (2). In terms of the displacement $y(t)$, Eq. (60) is equivalent to:

$$\ddot{y} + (C + \beta K_d)\dot{y} + \beta K_p y = \beta K_p r_0, \quad r_0 = 0.1. \tag{62}$$

Fig. 8(b) shows the measured step responses of the cart with $K_p = 60$ and $K_d = 0$ and with the reference displacement shown in Fig. 8(a). This reference response alternates from '0' position to 0.1 m. The voltage input for the measured step response $V_{in}(t)$ ranges from −2.3 V to 5.9 V with a mean of 0.3 V.

The response in Fig. 8(b) is underdamped but decays to zero rapidly, showing that there are significant non-linearities present. An initial approximation to this response is to assume the damping is constant. Thus the value of $\overline{C}$ in Eq. (60) and hence C in Eq. (62), are constant over time.

4.1.3. Constant damping

To identify C and β in Eqs. (55) and (56), parameters $\overline{C}$ and $\overline{\beta}$ are first identified and C and β are calculated from:

$$C = \overline{C} - \frac{\overline{\beta}}{K_p} K_d, \quad \beta = \frac{\overline{\beta}}{K_p}. \tag{63}$$

The experimental data used is the first step response of Fig. 8(b). The response is transformed into the measured error using Eq. (58) where $r(t) = r_0 = 0.1$ m. The starting time of $t = 0$ is taken to be the point that the cart velocity first goes non-zero in Fig. 8(b).

The algorithm of Fig. 6 is applied to the data in Fig. 8(b). The identified C and β are:

$$C_{60} = 6.1520 \quad \beta_{60} = 1.8545 \tag{64}$$

where the subscript '60' refers to the experimental gain K_p used to obtain the measured data. The resulting modeled response (solid) versus measured response (dots) is shown in Fig. 9. The constant damping model captures the measured response closely in the first peak, but start to deviate in the second peak, and does not capture the sudden decrease after 0.8 s. This error is due to not capturing the non-linear damping effects as the cart's velocity slows to zero and static friction dominates, which causes the common "dead-space" where a small voltage is not sufficient to move the cart.

4.1.4. Time varying damping

It is now assumed that the unknown damping parameter C in Eq. (55) varies across time step $\Delta t = 0.15$ s. This interval is again based on computing half the smallest zero crossing time interval $\Delta t_{1/2}$. As discussed earlier, this choice is essentially arbitrary but keeps the total number of damping values small for minimizing computation while ensuring that non-linear effects are captured sufficiently quickly. Applying the algorithm of Fig. 2 gives $\beta = 1.9352$ and a sequence of six values for $c(t)$ in Eq. (5) and is plotted in Fig. 10. Fig. 10 shows a net trend of increasing damping over time. Towards the latter part after 0.5 s, the damping is greater which corresponds to when the velocity

Please cite this article in press as: N. Wongvanich, et al., Minimal modeling methodology to characterize non-linear damping in an electromechanical system, Math. Comput. Simulation (2015), http://dx.doi.org/10.1016/j.matcom.2015.05.007

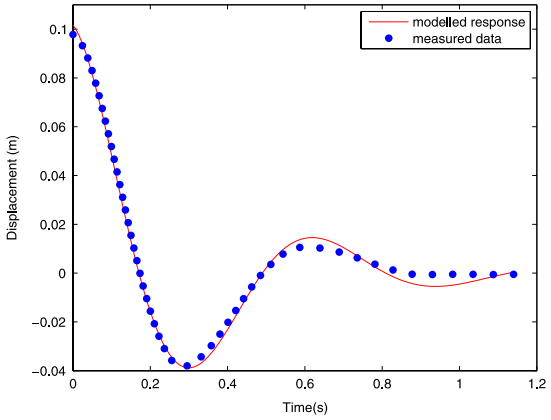

Fig. 9. Identified constant parameter modeled response (solid) versus measured error response (dotted) of cart for a step input of $r(t) = 0.1$ m.

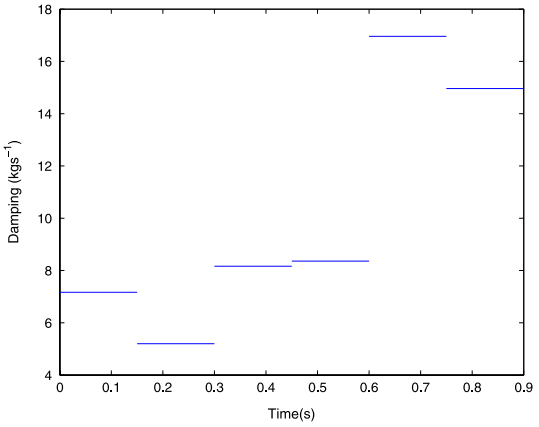

Fig. 10. Identified time varying damping $c(t)$ as defined in Eq. (5).

of the cart starts to significantly decrease so that static friction dominates. The jumps and "noise" in the damping values are due to the fact that several sections of the data in Fig. 9 are close to linear, for example, at between 0 and 0.16, and 0.32 and 0.48. To avoid these large jumps, and in accordance with Theorem 1 in the Analysis section, the algorithm of Fig. 2 is solved by linear least squares with the constraints:

$$c_1 - c_2 > \delta, \quad c_2 - c_3 > \delta, \ldots, c_5 - c_6 > \delta. \tag{65}$$

Fig. 11 shows the identified damping values for the choice of $\delta = 0.5$ in Eq. (65). The value of δ is chosen to be slightly positive to reflect the general trend of increasing damping over time as suggested by Fig. 11. Comparing Fig. 11 with Fig. 10 it can be seen that a similar damping trend is still present and for Fig. 11, $\beta = 1.9165$, as compared to $\beta = 1.9352$ without constraints. This 0.9% change shows that the voltage constant is essentially unaffected by the constraints of Eq. (65). Fig. 12(a) plots the resulting model matches for the cases of no constraints ($\delta = \infty$) and $\delta = 0.5$. The mean absolute displacement error for each case is 3.09 mm and 2.57 mm respectively, showing that the constraints have little effect on the overall response.

4.1.5. Damping as a function of velocity

Each damping value in Fig. 11 is defined over a constant interval of $\Delta t = 0.15$ s. An approximate representation of the velocity during each interval is the mean velocity $\overline{v_i}$, which is defined:

$$\overline{v_i} = \frac{1}{\Delta t} \int_{T_{i-1}}^{T_i} v(t) \mathrm{d}t, \quad i = 1, \ldots, 6. \tag{66}$$

Please cite this article in press as: N. Wongvanich, et al., Minimal modeling methodology to characterize non-linear damping in an electromechanical system, Math. Comput. Simulation (2015), http://dx.doi.org/10.1016/j.matcom.2015.05.007

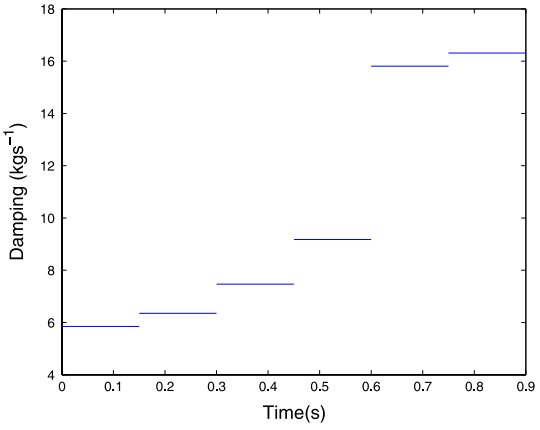

Fig. 11. Identified time varying damping $c(t)$ as defined in Eq. (5) for the choice of $\delta = 0.5$ in Eq. (65).

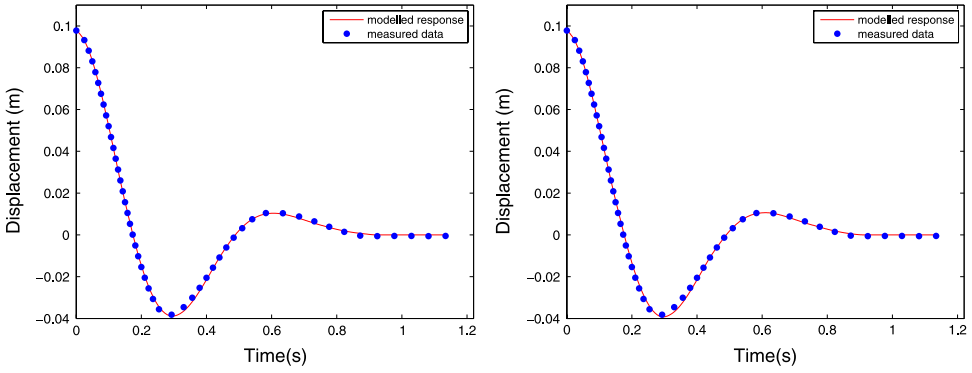

Fig. 12. (a) Model match for $\delta = \infty$ (no constraints) in Eq. (65) and (b) Model match for $\delta = 0.5$ in Eq. (65).

The values of $\overline{v_i}$, $i = 1, \ldots, 6$ are shown in Fig. 13. This mean velocity is then plotted against the corresponding damping values of Figs. 10 and 11 and is shown in Figs. 14(a) and (b). This result suggests an exponential model for relating damping to velocity:

$$C(v) = \alpha_1 e^{-\alpha_2 v} + \gamma. \tag{67}$$

Let $C_m(v)$ denote the measured damping versus velocity data in Figs. 14(a) and (b). Setting $C(v_i) = C_m(v_i)$ yields the equations:

$$\alpha_1 e^{-\alpha_2 v_i} = \overline{C}_m(v_i), \quad i = 1, \ldots, 6 \tag{68}$$

$$\overline{C}_m(v_i) = C_m(v_i) - \gamma. \tag{69}$$

Taking the natural logarithm of Eq. (68) yields:

$$A_1 - \alpha_2 v_i = \ln(\overline{C}_m(v_i)), \quad i = 1, \ldots, 6$$

$$A_1 = \ln(\alpha_1). \tag{70}$$

For a given estimate of γ, let $\alpha_{1,\gamma}$ and $\alpha_{2,\gamma}$ be the linear least squares solution to Eq. (68). Define:

$$F(\gamma) = \sum_{i=1}^{6} (\alpha_{1,\gamma} e^{-\alpha_{2,\gamma} v_i} + \gamma - C_m(v_i))^2. \tag{71}$$

Minimizing $F(\gamma)$ of Eq. (71) by non-linear regression in Matlab for each of the damping versus velocity curves in Fig. 14(a) gives the curves in Fig. 15.

Please cite this article in press as: N. Wongvanich, et al., Minimal modeling methodology to characterize non-linear damping in an electromechanical system, Math. Comput. Simulation (2015), http://dx.doi.org/10.1016/j.matcom.2015.05.007

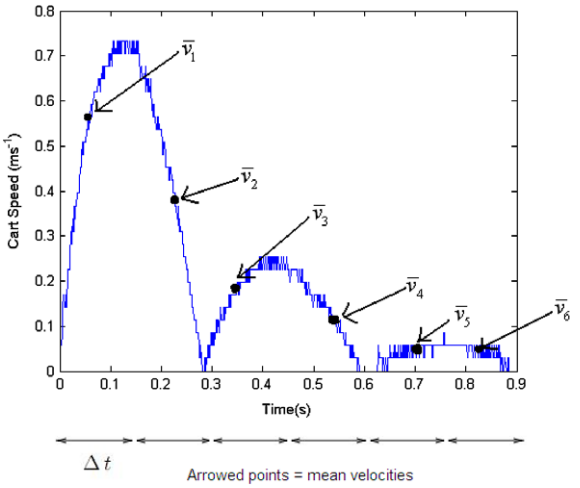

Fig. 13. A plot of the velocity against time with the mean velocity of each interval Δt where the piecewise damping $c(t)$ in Eq. (5) is defined over.

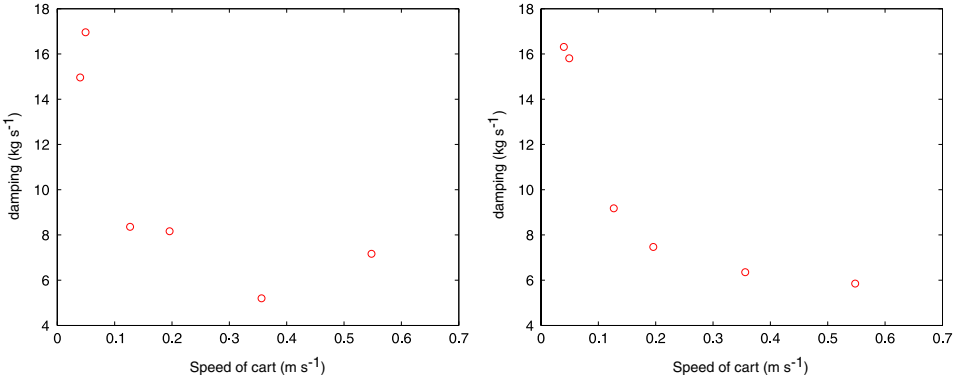

Fig. 14. (a) Damping versus velocity for $\delta = \infty$ in Eq. (65) and (b) Damping versus velocity for $\delta = 0.5$ in Eq. (65).

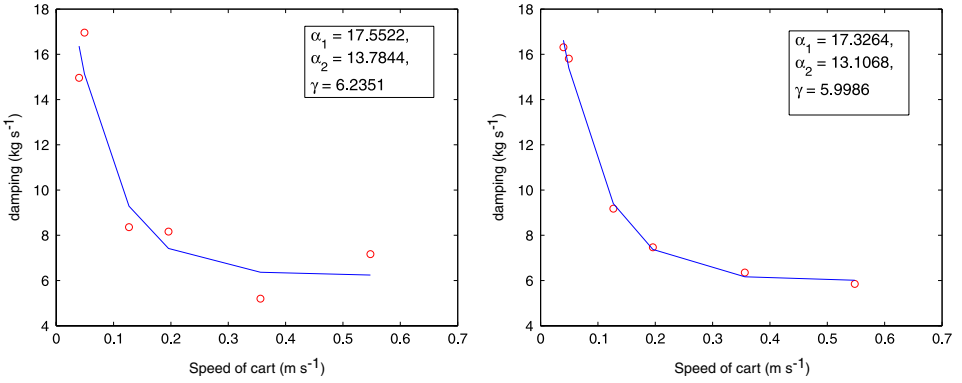

Fig. 15. (a) Best fit curve of Eq. (67) to the data in Fig. 14(a). (b) Best fit curve of Eq. (67) to the data in Fig. 14(b).

As shown by the α_1, α_2 and γ values in Figs. 15(a) and (b), the constraints of Eq. (65) do not have a major effect on the resulting damping versus velocity model of Eq. (67). Hence the algorithm of Fig. 2 provides a robust way of inferring a non-linear damping model. The final non-linear model of the error response (for the case of $\delta = 0.5$) in

Please cite this article in press as: N. Wongvanich, et al., Minimal modeling methodology to characterize non-linear damping in an electromechanical system, Math. Comput. Simulation (2015), http://dx.doi.org/10.1016/j.matcom.2015.05.007

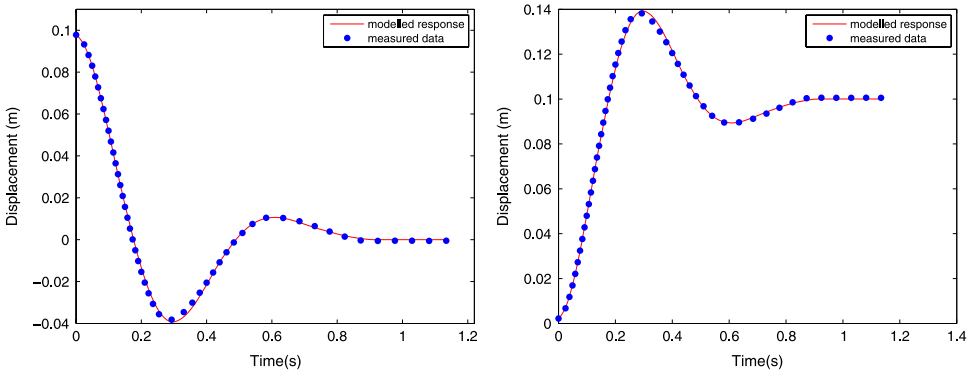

Fig. 16. (a) Identified non-linear model response (solid) of the cart from Eq. (72) against measured error response (dotted) and (b) Identified non-linear model response (solid) of the cart from Eq. (74) against measured cart displacement (dotted).

Eq. (60) is defined:

$$\ddot{e} + (\alpha_1 e^{-\alpha_2|\dot{e}|} + \gamma)\dot{e} + \overline{\beta} e = 0 \tag{72}$$

$$\alpha_1 = 17.3264, \quad \alpha_2 = 13.1068, \quad \gamma = 5.9986, \quad \beta_{60} = 1.9165. \tag{73}$$

The equivalent form of Eq. (72) in terms of the measured displacement is:

$$\ddot{y} + (\alpha_1 e^{-\alpha_2|\dot{y}|} + \gamma)\dot{y} + \overline{\beta}(y - r_0) = 0, \quad r_0 = 0.1. \tag{74}$$

The plots of the solution to Eqs. (72) and (74) are given in Figs. 16(a) and (b) which show a close match to the data. The modeled response in Fig. 16(a) captures the fast decay to zero quite closely and is significantly more accurate than the linear model of Fig. 8(b).

4.2. System identification with different proportional gains

To further test the algorithms of Figs. 2 and 6, they are applied separately to step error responses of the cart with $K_p = 80$ and $K_p = 100$. For $K_p = 80$, the voltage input range is [−4.0 V, 8.0 V], with a mean of 0.25 V. For $K_p = 100$, the voltage input range is [−6.1 V, 9.9 V], with a mean of 0.18 V. For the constant damping model, the algorithm of Fig. 6 is applied to the step error responses as was done for Fig. 9. The identified parameters are:

$$C_{80} = 5.4916, \quad \beta_{80} = 1.7482 \tag{75}$$

$$C_{100} = 4.5866, \quad \beta_{100} = 1.7866. \tag{76}$$

For the time varying damping model, the best fit exponential model are found for $K_p = 80$ and 100 from Eqs. (67)–(71) as was done for Figs. 15(a) and (b) with $K_p = 60$. The non-linear damping parameters for $K_p = 80$ and $K_p = 100$ are:

$$\alpha_{1,80} = 22.1357, \quad \alpha_{2,80} = 18.2233, \quad \gamma_{80} = 5.6035, \quad \beta_{80} = 1.9180, \tag{77}$$

$$\alpha_{1,100} = 15.2528, \quad \alpha_{2,100} = 5.9934, \quad \gamma_{100} = 3.7990, \quad \beta_{100} = 1.9100. \tag{78}$$

Fig. 17 shows the resulting exponential damping models superimposed with the damping model of Fig. 15(a). In addition, the β values are identified to be 1.9165, 1.9180, and 1.9100, for $K_p = 60$, 80 and 100 respectively.

The maximum deviations of the damping between the results of $K_p = 80$ and $K_p = 100$ as compared to $K_p = 60$ are 17.53% for the speed less than 0.4 m/s and 22.68% for the speed greater than 0.4 m/s. This greater error for the higher speeds is largely due to the last data points at 0.8 m/s in the $K_p = 100$ case. No such data points exist for the lower gains as the cart did not move as fast in these cases which would be expected since the control force was smaller. However, the overall results demonstrate that the identified damping models are quite similar for different proportional gains, and the stiffnesses β are essentially unchanged. This result of Fig. 17 is an important validation as the three different sets of K_p gains 60, 80, and 100 give three very different cart responses, with voltage input ranges of [−2.3 V, 5.9 V], [−4.0 V, 8.0 V] and [−6.1 V, 9.9 V] respectively. Yet, similar damping values and virtually

Please cite this article in press as: N. Wongvanich, et al., Minimal modeling methodology to characterize non-linear damping in an electromechanical system, Math. Comput. Simulation (2015), http://dx.doi.org/10.1016/j.matcom.2015.05.007

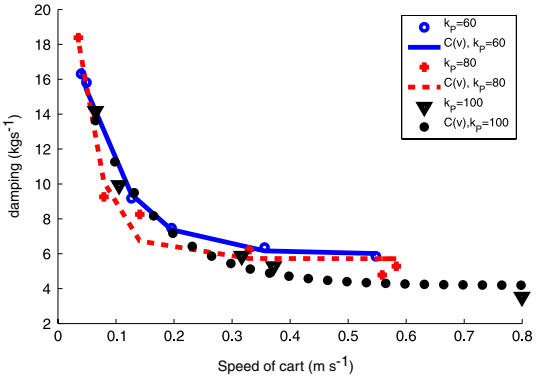

Fig. 17. Resulting exponential models for $K_p = 80$ and 100 superimposed onto the identified damping parameter model of Fig. 15(a).

identical β values are obtained. In contrast, for the linear damping model, the values of β vary significantly more from 1.75 to 1.85 which shows that the modeling error in the damping is partly compensated by changing β.

For the purposes of comparison, define three different linear models Lm_1, Lm_2, Lm_3 as follows:

$$Lm_1 \equiv \text{solution to Eq. (62) with } C = C_{60} \text{ and } \beta = \beta_{60} \text{ from Eq. (64) and arbitrary gains } K_p \text{ and } K_d, \tag{79}$$

$$Lm_2 \equiv \text{solution to Eq. (62) with } C = C_{80} \text{ and } \beta = \beta_{80} \text{ from Eq. (75) and arbitrary gains } K_p \text{ and } K_d \tag{80}$$

$$Lm_3 \equiv \text{solution to Eq. (62) with } C = C_{100} \text{ and } \beta = \beta_{100} \text{ from Eq. (76) and arbitrary gains } K_p \text{ and } K_d. \tag{81}$$

Similarly, three non-linear models NLm_1, NLm_2 and NLm_3 are defined:

$$NLm_1 \equiv \text{solution to Eq. (62) with } \beta = \beta_{60} \text{ and } C = C(v) \text{ from (67), with } \alpha_1 = \alpha_{1,60}, \alpha_2 = \alpha_{2,60}, \gamma = \gamma_{60} \text{ from (73)} \tag{82}$$

$$NLm_2 \equiv \text{solution to Eq. (62) with } \beta = \beta_{80} \text{ and } C = C(v) \text{ from (67), with } \alpha_1 = \alpha_{1,80}, \alpha_2 = \alpha_{2,80}, \gamma = \gamma_{80} \text{ from Eq. (77)} \tag{83}$$

$$NLm_3 \equiv \text{solution to Eq. (62) with } \beta = \beta_{100} \text{ and } C = C(v) \text{ from (67), with } \alpha_1 = \alpha_{1,100}, \alpha_2 = \alpha_{2,100}, \gamma = \gamma_{100} \text{ from Eq. (78).} \tag{84}$$

The models of Lm_1, Lm_2, Lm_3 in Eqs. (79)–(64) and NLm_1, NLm_2 and NLm_3 in Eqs. (82)–(84) can be used to test any sets of gains K_p and K_d in Eq. (62).

Figs. 18(a) and (b) show the resulting model matches to the experimental data for the non-linear models NLm_2 and NLm_3 and the constant damping models Lm_2 and Lm_3. These plots illustrate that the non-linear model captures the measured dynamics significantly more accurately than the constant damping model, as was the case with Fig. 16(a). The mean absolute error in the displacement in Fig. 18(a) are 7.1 mm for the linear model Lm_2 and 1 mm for the non-linear model NLm_2. For Fig. 18(b), the mean errors are 7.4 mm for the linear model Lm_3 and 1.7 mm for the non-linear model NLm_3. Thus, in both cases the fitting error is reduced by a factor of 7.

4.3. PD control response predictions

A final proof-of-concept is to test the ability of the linear and non-linear identified response models to predict PD control responses to a reference step input $r(t) = 0.1$ m for a number of different gains. The voltage inputs to the control responses are given in Table 1 which shows a significant range of values.

Please cite this article in press as: N. Wongvanich, et al., Minimal modeling methodology to characterize non-linear damping in an electromechanical system, Math. Comput. Simulation (2015), http://dx.doi.org/10.1016/j.matcom.2015.05.007

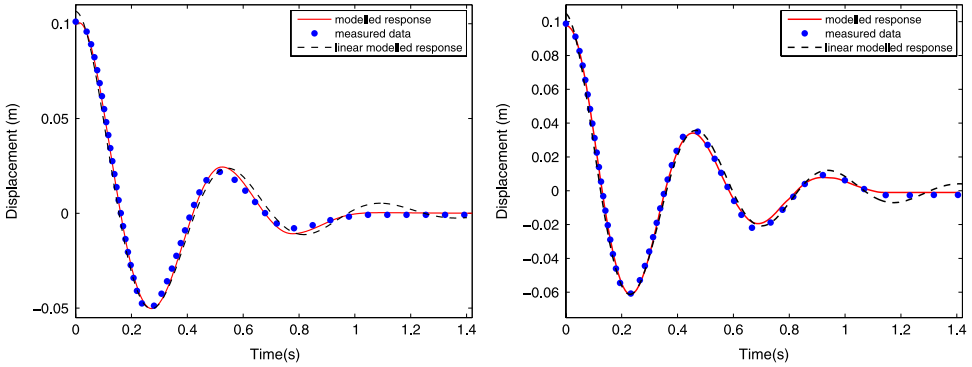

Fig. 18. (a) Model matches to experimental data for $K_p = 80$ and (b) Model matches to experimental data for $K_p = 100$.

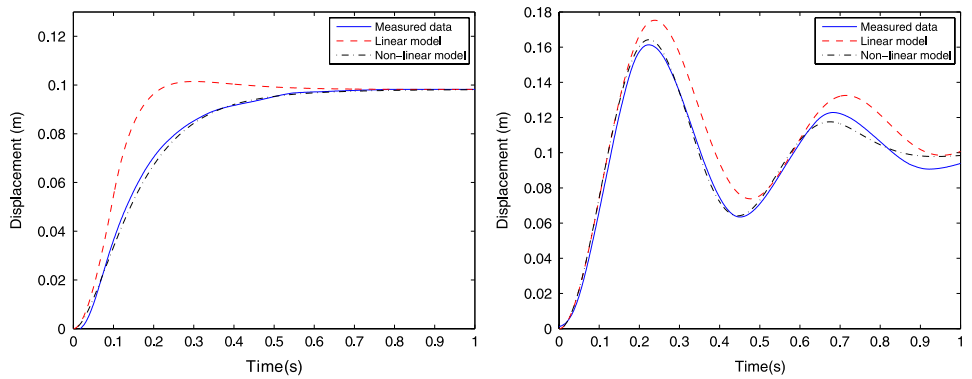

Fig. 19. (a) Predicted responses for the case of $K_p = 80$, $K_d = 10$ using Lm_2 of Eq. (80) and NLm_2 of Eq. (83) and (b) Predicted responses for the case of $K_p = 100$, $K_d = 0$ using Lm_3 and NLm_3.

Table 1
Voltage inputs to the control responses prediction data.

K_p	K_d	Min. Voltage (V)	Mean voltage (V)	Max. Voltage (V)
60	0	−2.30	0.31	5.87
60	5	−0.44	0.55	12.0
80	0	−4.05	0.25	8.08
80	5	−1.23	0.96	12.0
80	10	−0.49	0.59	12.0
100	0	−6.13	0.18	9.88
100	5	−2.05	0.43	12.0
100	10	−1.90	0.43	12.0

Figs. 19(a) and (b) show that the non-linear damping model NLm_1 significantly outperforms the constant damping model Lm_1. Table 2 gives the mean absolute error between the measured and model responses for a number of PD control experiments using the six models Lm_1, Lm_2, Lm_3, NLm_1, NLm_2 and NLm_3 from Eqs. (79)–(84) over 1 s of experimental data. On average, the non-linear model NLm_1 has an error of 2.2 mm which is much smaller than the linear model Lm_1 prediction error of 5.8 mm. Similarly, the non-linear models NLm_2 and NLm_3 have average errors of 2.2 mm and 2.7 mm which are much smaller than the corresponding errors for the linear models Lm_2 and Lm_3 which are 6.0 mm and 6.6 mm. Furthermore, Table 2 also gives the mean absolute error averages over experimental data of 0.5 s. These averages provide more accurate comparison between the linear and non-linear models, since the 1 s average includes half the time at which the system spends at steady state. Over 0.5 s, the non-linear models NLm_1, NLm_2, and NLm_3 incur average errors of 2.9 mm, 2.8 mm and 3.1 mm; which are much smaller than the linear model Lm_1, Lm_2, and NLm_3 prediction errors of 7.8 mm, 9.0 mm and 9.6 mm respectively. In addition, the spread of errors

Please cite this article in press as: N. Wongvanich, et al., Minimal modeling methodology to characterize non-linear damping in an electromechanical system, Math. Comput. Simulation (2015), http://dx.doi.org/10.1016/j.matcom.2015.05.007

Table 2
Percentage error comparison of the linear and non-linear models for each set of PD gains using three different model characterizing sets.

PD control responses		Constant damping model			Non-linear model		
K_p	K_d	Lm_1 (mm)	Lm_2 (mm)	Lm_3 (mm)	NLm_1 (mm)	NLm_2 (mm)	NLm_3 (mm)
60	0	7	9.7	11	1	3.4	4.1
60	5	6	6.3	7.2	3.3	3.9	3.6
80	0	6.9	7.1	7.4	2	1.1	2.5
80	5	3.3	2.7	4.1	1.9	1.4	2.7
80	10	7	4.6	8.0	2	1.4	2.4
100	0	7.9	9.5	7.4	4.1	2.9	3.6
100	5	2.6	2.6	2.3	1.5	1.4	1.1
100	10	5.6	6.0	5.2	2	2.4	1.7
Average error (1 s)		5.8	6.0	6.6	2.2	2.2	2.7
Average error (0.5 s)		7.8	9.0	9.6	2.9	2.8	3.1

for the non-linear model over 1 s is from ∼1 mm to 4 mm where the spread of errors in the linear model over 1 s is from ∼2 mm to 7 mm.

Hence, for the non-linear case, equally good models are obtained regardless of specific experimental data used to identify the parameters. For the linear case, predictions are significantly more affected by the model generating data set chosen. This result further validates the time varying damping method presented in this paper.

4.4. Practical controller design

To further prove the importance of the non-linear model in control design, a simple PD controller is constructed based on the following specifications:

$$\text{Given } K_p = 100, \text{ minimize } K_d \text{ such that settling time } (1\%) \leq 0.5\text{s}. \tag{85}$$

These specifications in Eq. (85) are met with both the linear model Lm_3 of Eq. (81) and the non-linear model NLm_3 of Eq. (84).

For the linear model the K_d gain was computed to be 7.35 and for the non-linear model, the K_d gain was 3.55. Hence, for this example, the derivative gain for the linear approach was more than twice the non-linear. In practice, this result of a higher derivative gain, would require significantly more smoothing on the data to avoid the derivative control over-responding to noise, which would in turn create more time lag further affecting control. In other words, the smaller the K_d gain designed to meet the specifications, the more effective and easier to implement, the controller will be. In addition, the control input required for the non-linear model is significantly less than the control input for the linear model. Specifically, the mean squared voltage input was 3.0V^2 and 2.0V^2 for the linear and non-linear models respectively. Hence these results demonstrate the importance of characterizing the non-linear dynamics of the system.

Consider Fig. 19(a). The experimental PD controller in this case was designed using the linear model to have an overshoot of 1% and a rise time of less than 0.18 s. However, the experimental result had no overshoot and a significantly longer rise time of 0.5 s. This is an error of 278% which would not normally be acceptable in control design. The non-linear model on the other hand predicted this result very closely with a rise time of 0.49 s and no overshoot so would have avoided this poor control design.

Finally, Fig. 20 shows the result of designing a controller based on the non-linear model with an overshoot of 0.1% and rise time of 0.3 s. The experimental result for this design gave no overshoot and rise time of 0.3 s, which is a very close match. Using the same parameters, the linear model would have predicted an overshoot of 2% and rise time of 0.21 s, that is significantly different.

In summary, these examples prove that adding non-linear dynamics has a major effect on the accuracy of predicting control system response based on a very small number of experiments. If further experiments were used, a linear model could be made to work, but at the cost of more experiments. This is an important concept to demonstrate, as in applications like machine control [4] and manufacturing [7], the extra testing would increase costs and turn around time.

Please cite this article in press as: N. Wongvanich, et al., Minimal modeling methodology to characterize non-linear damping in an electromechanical system, Math. Comput. Simulation (2015), http://dx.doi.org/10.1016/j.matcom.2015.05.007

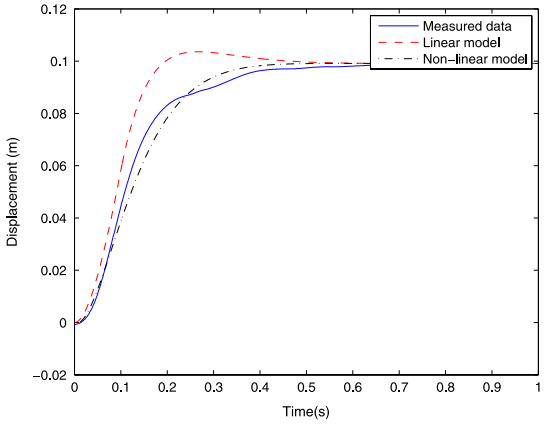

Fig. 20. Controller design responses for $Lm1$ of Eq. (79) and $NLm1$ of Eq. (84).

4.5. Comparison to non-linear regression

4.5.1. Constant damping model

A final test of the method is to compare the computational efficiency and accuracy versus standard non-linear regression. For the constant damping model of Eq. (62), non-linear regression is then used to match the model to the data using standard functions in Matlab, with the starting point of $C = 1, \beta = 1$; to create a numerical solution. For comparison, non-linear regression is also used to match the analytical solution of the differential equation of Eq. (62) to the data, as defined:

$$y_{\text{analytical}} \equiv \frac{(2y_0' + cy_0)}{\omega} \exp(-\tfrac{1}{2}Ct)\sin(\tfrac{1}{2}\omega t) + y_0 \exp(-\tfrac{1}{2}Ct)\cos(\tfrac{1}{2}\omega t), \tag{86}$$

$$\omega = \sqrt{4\beta K_p - C^2}, \quad K_p = 60 \tag{87}$$

$$N \equiv \text{ number of data points.} \tag{88}$$

The final parameters were found to be:

$$C = 6.72, \quad \beta = 1.81. \tag{89}$$

The resulting model is compared to the measured cart data with $K_p = 60$, $K_d = 0$ in Fig. 21, which shows a reasonable match but significant errors build up towards the end of the data when non-linearities become significant. The absolute error of the modeled response compared to the measured was 0.006 m, which is close to the value of 0.0072 m found by the proposed method of Fig. 6 as given in Fig. 9. Hence in terms of accuracy, there is little difference between the methods for the constant damping case.

4.5.2. Time varying damping model

The piecewise damping model of Eqs. (4)–(7) is used with $n = 6$, with non-linear regression being applied using standard functions in Matlab, to construct a numerical solution. For comparison, a piecewise analytical solution is constructed to Eq. (62) with $c = c(t)$ the piecewise constant approximation defined by Eqs. (5) and (6) with $n = 6$. This analytical solution is defined:

$$\begin{aligned} y_{analytical}(t) &= y_{soln,1}(t), \quad t \in T_0 < t < T_1 \\ &= \vdots \\ &= y_{soln,n}(t) \quad t \in T_{n-1} < t < T_{end} \end{aligned} \tag{90}$$

Please cite this article in press as: N. Wongvanich, et al., Minimal modeling methodology to characterize non-linear damping in an electromechanical system, Math. Comput. Simulation (2015), http://dx.doi.org/10.1016/j.matcom.2015.05.007

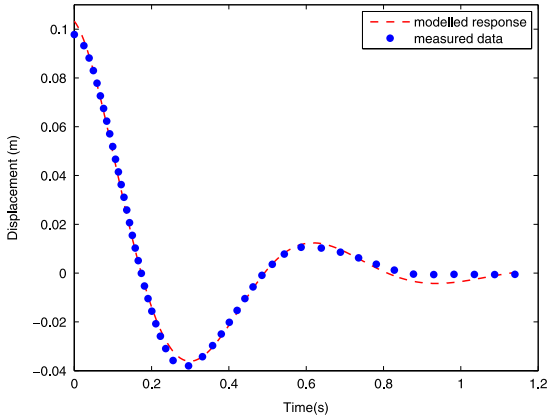

Fig. 21. Comparison of the linear modeled response (dotted) via Non Linear Regression modeling against the actual response (solid) for a step input.

Table 3
Computational load comparison between non-linear regression and the proposed integral method of Section 2.

Identification method	Computational time (s)
Non-Linear Regression (linear model)	1.52 (`ode45`), 0.07 (analytical)
Non-Linear Regression (time varying, linear model starting) (time varying, $c_1 = \cdots = c_6 = 100$, $\beta = 100$)	 54.7 (`ode45`), 0.28 (analytical) 128.3 (`ode45`), 0.60 (analytical)
Constant Parameter Integral method	0.001
Time Varying Parameter Integral method	0.007

where:

$$y_{soln,i}(t) = \frac{(2y'_{i-1} + c_i y_{i-1})}{\omega_i} \exp(-\tfrac{1}{2}c_i(t - T_i)) \sin(\tfrac{1}{2}\omega_i(t - T_i)) + y_{i-1} \exp(-\tfrac{1}{2}c_i(t - T_i)) \cos(\tfrac{1}{2}\omega_i(t - T_i)), \quad i = 1, \ldots, 6 \tag{91}$$

$$\omega_i = \sqrt{4\beta K_p - c_i^2}, \quad K_p = 60, \quad i = 1, \ldots, 6. \tag{92}$$

Note that an analytical solution may not always be available, hence both approaches are included for analysis. As a starting point the values $c_1 = c_2 = \cdots = c_6 = c$ and β are used from Eq. (89), which correspond to the linear model. The mean absolute error for the time varying model is 1.0 mm. Thus the algorithms of Figs. 2 and 6 and non-linear regression give similar accuracy.

Table 3 shows the results of computational speed comparison of the proposed method of Fig. 6 versus non-linear regression. In each case the time required to load the experimental data is not included and simulations were done in Matlab using Intel ®CORE 2 Duo processor desktop, with 2.0 GHz CPU and 2.0 GB of RAM. For the linear damping, the integral method is 70 times faster than non-linear regression for the analytical formulation and 1520 times faster than the numerical formulation. For the time varying damping, the integral method is 40 times faster than non-linear regression for the analytical formulation, and 7800 times faster than numerical formulation. In this case, for a starting point far away from the solution, the integral method is 86 times and 18300 times faster than non-linear regression for the analytical and numerical formulations respectively. This shows the typical starting point dependence of standard non-linear regression. The integral method does not have this issue as the starting point is the data itself, which by definition is already close to the solution. The proposed method also only requires linear least squares and involves integrals which are sums of the data and thus very fast to compute. Furthermore, the integral method does not require a solution to the underlying differential equation model of Eq. (4), where a typical non-linear regression would solve Eq. (4) at each iteration.

Please cite this article in press as: N. Wongvanich, et al., Minimal modeling methodology to characterize non-linear damping in an electromechanical system, Math. Comput. Simulation (2015), http://dx.doi.org/10.1016/j.matcom.2015.05.007

5. Conclusion

A general modeling methodology for non-linear damping in second order systems is developed. The method using a piecewise constant model of damping and relates the identified values to the absolute value of velocity by a decaying exponential function. An analytical proof shows that this approach is uniquely identifiable under the constraint that the derivative of the damping is bounded. The exponential decay of the damping versus speed reveals the increased friction or "stiction" that occurs at small velocities and also includes the dynamics of gear backlash. There are many quite complex models in the literature for capturing this behavior of the static friction, gear backlash and other non-linearities in a DC motor and electro-mechanical systems. However, the methods typically make strong initial assumptions on the model then match this model to the data. The approach in this paper is to initially start with simplified models and add complexity as required to better predict experimental responses.

The non-linear method accurately predicted a range of PD controlled responses with only one data set used to identify the model and provided a significant improvement over the linear method. In addition, a PD control design experiment showed that the non-linear approach required less than half the derivative gain to meet the same specifications, resulting in a better controller. These examples validate the importance of including non-linear damping for control system prediction and design in this cart system. Overall it demonstrates the concept of using a non-linear model to significantly minimize the number of experiments required in PD tuning as compared to a standard linear modeling approach. This concept differs to the usual approach, which is to let the controller itself deal with the modeling error. A complex control algorithm may potentially minimize experiments and allow linear models to work, but the control algorithm would then hide potentially predictable dynamics that could simplify implementation. In any practical system, the simpler the control method the less chance of coding errors and hardware failures hence the more reliability.

Finally, the identification algorithm was shown to be up to 7800 times faster than standard non-linear regression showing that it has very minimal computation requirements and is thus a useful tool for modeling second order systems.

Appendix. Proofs

Proof of Theorem 1.

Proof. First, consider the case at $t = 0$. Assume that the following statement is true:

$$\exists\, \bar{N} \text{ and } \delta > 0 \text{ such that } \forall\, k > \bar{N}, |F_{model,k}(0) - F_{true}(0)| > \delta. \tag{A.1}$$

Since the derivative of F_{true} and the derivative of F_{model} are bounded, it will take a finite time independent of k before $F_{true}(t)$ and $F_{model,k}(t)$ intersect. Thus, $\exists\, dt^* > 0$ and $\delta^* > 0$ such that:

$$F_{model,k}(t) - F_{true}(t) > \delta^*, \text{ or } F_{true}(t) - F_{model,k}(t) > \delta^*, \quad \forall t \in [0, dt^*],\ \forall k > \bar{N}. \tag{A.2}$$

Furthermore, since $y'_{true}(0) < 0$ independent of k, $\bar{dt}^* < dt^*$ can be chosen sufficiently small so that $\dot{y}_{true}(t) < 0, \forall t \in [0, dt^*]$. From Eq. (A.2), $F_{model,k}(t) - F_{true}(t)$ cannot change sign on the interval $t \in [0, dt^*]$ hence:

$$\begin{aligned}\left|y_{true}(\bar{dt}^*) - y_{model,k}(\bar{dt}^*)\right| &= \left|\int_0^{\bar{dt}^*}\int_0^{\tau}\Big(F_{model,k}(s) - F_{true}(s)\Big)\dot{y}_{true}\, ds\, d\tau\right| \\ &= \int_0^{\bar{dt}^*}\int_0^{\tau}\left|\Big(F_{model,k}(s) - F_{true}(s)\Big)\right|\,|\dot{y}|\, ds\, d\tau \\ &= \delta^*\int_0^{dt^*}\int_0^{\tau}|\dot{y}|\, ds\, d\tau = \delta^{**} > 0, \quad \forall k > \bar{N}.\end{aligned} \tag{A.3}$$

However, Eq. (A.3) contradicts Eq. (48). Therefore, Eq. (A.2) is a false statement and thus $F_{model,k}(0) \to F_{true}(0)$ as $k \to \infty$.

The next step is to prove convergence for a non-zero time. Let $t_0 > 0$ be the smallest time where convergence of Eq. (50) does not hold. Hence $\exists\, \bar{N}$ and $\delta > 0$ such that:

$$|F_{model,k}(t_0) - F_{true}(t_0)| > \delta,\ \forall k > \bar{N}. \tag{A.4}$$

Please cite this article in press as: N. Wongvanich, et al., Minimal modeling methodology to characterize non-linear damping in an electromechanical system, Math. Comput. Simulation (2015), http://dx.doi.org/10.1016/j.matcom.2015.05.007

In a similar way to the $t = 0$ case, because of the bound on the derivatives of F_{true} and $F_{model,k}$, $\exists\ dt^* > 0$ and $\delta^* > 0$ such that:

$$F_{model,k}(t) - F_{true}(t) > \delta^* \quad t \in [t_0^-, t_0^+], \quad \forall k > \bar{N} \tag{A.5}$$

$$t_0^- = t_0 - dt^*, \quad t_0^+ = t_0 + dt^*. \tag{A.6}$$

However, Eq. (A.6) implies that $\exists\ t < t_0$ where convergence of Eq. (49) does not hold which contradicts the assumption that t_0 is the smallest such value. Thus, no $t_0 > 0$ exists where Eq. (50) does not hold and therefore Eq. (50) must be true for all t. □

Proof of Corollary 2.

Proof. Define the piecewise constant model:

$$\bar{C}_{i,model}^{(k)} = \frac{F_{true}(\Delta t\, i) + F_{true}(\Delta t\, (i-1))}{2}, \quad i = 1, \ldots, k, \quad \Delta t = \frac{1}{k} \tag{A.7}$$

$$\bar{F}_{model,k}(t) \equiv F_{model,k}(t) \text{ in Eq. (44) with } C_{i,model}^{(k)} = \bar{C}_{i,model}^{(k)} \tag{A.8}$$

$$\bar{y}_{model,k}(t) \equiv y_{model,k}(t) \text{ in Eq. (45) with } F_{model,k} = \bar{F}_{model,k}. \tag{A.9}$$

From Eq. (A.7) it follows that:

$$\lim_{k\to\infty} \bar{F}_{model,k}(t) = F_{true}(t), \quad \forall t \in [0, T_{end}]. \tag{A.10}$$

Replacing $y_{model}(t)$ in Eq. (35) by $\bar{y}_{model,k}(t)$ in Eq. (A.9), shows that $\bar{y}_{model,k}(t) \to y_{true}(t)$ as $k \to \infty$.

However, by definition of linear least squares:

$$\int_0^{T_{end}} \left(\int_0^t \int_0^t \left(F_{model,k}^* - F_{true}\right)^2 dt\, dt \right) dt \le \int_0^{T_{end}} \left(\int_0^t \int_0^t \left(\bar{F}_{model,k} - F_{true}\right)^2 dt\, dt \right) dt \ \forall k. \tag{A.11}$$

Since the right hand side of Eq. (A.11) $\to 0$ as $k \to \infty$, Eq. (49) follows. □

References

[1] Y. Ando, M. Suzuki, Control of active suspension systems using the singular perturbation method, Int. J. Robot. Res. 4 (1996) 287–293.
[2] P. Barone, Some practical remarks on the extended prony's method of spectrum analysis, Proc. IEEE 76 (1988) 716–723.
[3] K. Chopra, Dynamics of Structures: Theory and Application to Earthquake engineering, third ed., Pearson Prentice Hall, Upper Saddle River, 2007.
[4] J. Dhupia, A.G. Ulsoy, Control of Machine Tools and Machining Processes, in: The Control Handbook: Control System Applications, CRC Press, Boca Raton, 2011.
[5] J.-L. Dion, S.L. Moyne, G. Chevallier, H. Sebbah, Gear impacts and idle gear noise: Experimental study and non-linear dynamic model, Mech. Syst. Sig. Process. 23 (2009) 2608–2628.
[6] S. Ge, L. Huang, T. Lee, Position control of chained multiple mass–spring–damper systems adaptive output feedback control approaches, Int. J. Control. Autom. 2 (2004) 144–155.
[7] C. Hann, D. Atchison, D. Kirk, E. Brouwers, Modelling and system identification of a stiff stay wire fence machine, Proc. Inst. Mech. Eng., B J. Eng. Manuf. 226 (2010) 1069–1083.
[8] C. Hann, J.G. Chase, Y.M. F., J. Elfring, N.M. Nor, P. Lawrence, G. Shaw, The impact of parameter identification methods on drug therapy control in an intensive care unit, Open Med. Inform. J. 2 (2008) 92–104.
[9] C. Hann, I. Singh-Levett, B. Deam, J. Mander, J.G. Chase, Real-time system identification of a nonlinear four-storey steel frame structure—application to structural health monitoring, IEEE Sens. J. 9 (2009) 1339–1346.
[10] C. Hann, M. Snowdon, A. Rao, O. Winn, N. Wongvanich, X. Chen, Minimal modelling approach to describe turbulent rocket roll dynamics in a vertical wind tunnel, Proc. Inst. Mech. Eng. G J. Aerosp. Eng. 226 (2011) 1042–1060.
[11] C.E. Hann, J. Chase, J. Lin, T. Lotz, C. Doran, G. Shaw, Integral-based parameter identification for long-term dynamic verification of a glucose-insulin system model, Comput. Meth. Programs Biomed. 77 (2005) 259–270.
[12] S. Hannot, D. Rixen, Building and reducing a three-field finite-element model of a damped electromechanical actuator, J. Microelectromech. Syst. 20 (2011) 665–675.
[13] J. Humar, Dynamics of Structures, A.A. Balkena Publishers, Lisse, The Netherlands, 2002.
[14] S. Kay, S. Saha, Mean likelihood frequency estimation, IEEE Trans. Signal Process. 48 (2000) 1937–1946.
[15] T. Kim, T.E. Rook, R. Singh, Super-and subharmonic response calculations for a torsional system with clearance nonlinearity using the harmonic balance method, J. Sound Vib. 281 (2005) 965–993.

Please cite this article in press as: N. Wongvanich, et al., Minimal modeling methodology to characterize non-linear damping in an electromechanical system, Math. Comput. Simulation (2015), http://dx.doi.org/10.1016/j.matcom.2015.05.007

[16] R. Kumaresan, D. Tufts, Estimating the parameters of exponentially damped sinusoids and pole-zero modeling in noise, IEEE Trans. Acoust., Speech, Signal Process 30 (1982) 833–840.
[17] D. Lam, H. Yee, B. Campbell, An efficient improvement of the aesops algorithm for power system eigenvalue calculation, IEEE Trans. Power Syst. 9 (1994) 1880–1885.
[18] V. Lu, Y.K. Cheung, Non-linear vibration analysis of multilayer beams by incremental finite elements, part ii: Damping and forced vibrations, J. Sound Vib. 100 (1982) 373–382.
[19] R. McGowan, C. Smith, C. Browman, B.A. Kay, Methods for least-squares parameter identification for articulatory movement and the program parfit, Haskin Lab Status Rep. Speech Res. SR-101/102, 1990, pp. 220–230.
[20] J. Mills, D. Lokhorst, Control of robotic manipulators during general task execution: a discontinuous control approach, Int. J. Robot. Res. 12 (1993) 146–163.
[21] R. Nelson, Flight Stability and Automatic Control, second ed., McGraw Hill, New York, 1998.
[22] R. Oosterbaan, Frequency and regression analysis, IILRI 16 (1994) 175–224.
[23] S. Rao, Mechanical Vibrations, Addington Wesley, 2002.
[24] C. Ray, Z. Huang, Power grid dynamics: Enhancing power system operation through prony analysis, US DOE J Undergraduate Res. VII, 2007, pp. 87–90.
[25] Y.M. Sam, J.H.S. Osman, Modeling and control of the active suspension system using proportional–integral sliding mode approach, Asian J. Control 7 (2005) 91–98.
[26] B.F. Spencer, S. Dyke, M. Sain, J. Carlson, Phenomenological model of a magnetorheological damper, J. Eng. Mech. 123 (1997) 230–238.
[27] C. Starfinger, C. Hann, J. Chase, T. Desaive, A. Ghuysen, G.M. Shaw, Model-based cardiac diagnosis of pulmonary embolism, Comput. Meth. Programs Biomed. 87 (2007) 46–60.
[28] N. Uchida, T. Nagao, A new eigen-analysis method of steady-state stability studies for large power systems: S matrix method, IEEE Trans. Power Syst. 3 (2007) 706–714.
[29] A. Velotsos, C. Ventura, Modal analysis of non-classically damped linear systems, Earthq. Eng. Struct. D. 14 (1986) 217–243.
[30] Y. Wen, Method of random vibration of hysteretic systems, J. Eng. Mech-ASCE 2 (1976) 249–263.
[31] R.A. Wiltshire, G. Ledwich, P. O'Shea, A kalman filtering approach to rapidly detecting modal changes in power systems, IEEE Trans. Power Syst. 22 (2007) 1698–1706.
[32] P. Wolm, X. Chen, J. Chase, W. Pettigrew, C. Hann, Analysis of a pm dc motor model for application in feedback design for electric-powered mobility vehicles, Int. J. Comput. Appl. Technol. 39 (2010) 116–122.

Please cite this article in press as: N. Wongvanich, et al., Minimal modeling methodology to characterize non-linear damping in an electromechanical system, Math. Comput. Simulation (2015), http://dx.doi.org/10.1016/j.matcom.2015.05.007